SIMULATION OF ARC MOTION IN ALTERNATING MAGNETIC FIELD USING DIMENSIONLESS MOMENTUM EQUATION

K. Takeda*, R. Akiho

Faculty of Systems Science and Technology, Akita Prefectural University, Yuri-Honjyo, Akita, 015-0055, Japan

* ktkd@ruby.ocn.ne.jp

Abstract. A new heat-treatment system has been developed using an arc driven by an alternating magnetic field. The arc motion was theoretically investigated by the method of non-dimensional analysis. After the definition of the pertinent characteristic length and time, the momentum equation was converted into the dimensionless form. This approach gave us not only a short cut to simulate the arc motion but also clear understanding on the nature of the magnetically driven arc.

Keywords: heat treatment, arc motion, magnetic field, momentum equation, non-dimensional analysis.

1. Introduction

When an alternating magnetic field is applied perpendicularly to an arc, the arc swings back and forth like a pendulum [1–3]. The authors refer to such an arc as a magnetically driven arc. The magnitude of the arc power and the amplitude of its oscillatory motion can be adjusted by changing the arc current and the applied field strength, respectively. The heat flux distribution can be controlled by changing the wave form of the alternating field. As shown in Figure 1, the distribution of the heat flow is rather flat for the sinusoidal wave form. While for the rectangular wave form, heat flows are concentrated at the both ends of the oscillation amplitude.

Using the magnetically driven arc, a new heat treatment system has been developed. As shown in Figure 2, it is composed of several sections. A transferred dc arc burns between a plasma torch and a work piece which serves as an anode. Various types of alternating magnetic field could be produced by an ac current supply. The work piece travells at any arbitrary velocity in horizontal direction by a driving mechanism of an anode platform. After the heating, it is quenched by cooling water sprayed from its back side. The sequences of the treatment are proceeded automatically by a programmable logic controller. To check the performance of the treatment, Vickers hardness tests were carried out. The test for the carbon steel after the heat treatment revealed that the hardness increased more than three times compared to the initial one [4].

To expand the application of this heat treatment, it is important to know the exact behaviours of the arc under various operating conditions. Few investigations were carried out for various alternating magnetic fields [5, 6]. As the arc motion depends on many operating parameters, it is not easy to understand the nature of the arc. The aim of the present work is to open a simple way to simulate the arc motion using a dimensionless analysis. In the following section, the governing equation will be prepared together with nec-
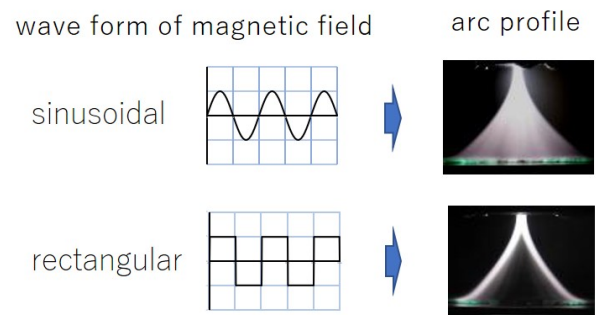

Figure 1. Control of the heat flow distribution by changing the wave form of the magnetic field.
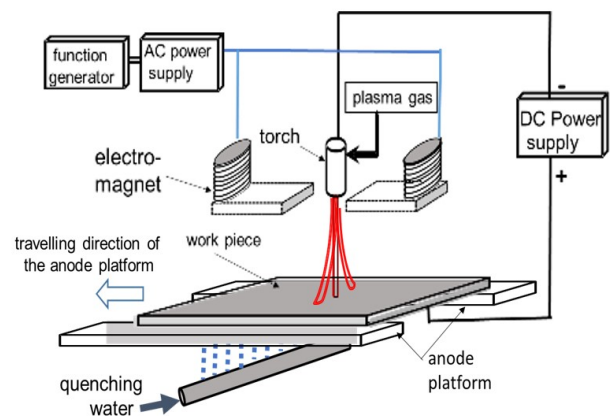

Figure 2. Arrangement of the developed heat treatment system.

essary initial conditions. In Section 3, a new approach using non-dimensional analysis will be discussed to solve the governing equation. Numerical calculations will be carried out in Sections 4 and 5. To confirm the theoretical predictions, experimental observation will be reported also in Section 5. Summary talk will be presented in Section 6.

Main parameters and their symbols used in this article are listed in Table 1 .

symbol	nomenclature
B	magnetic flux density (vector)
B	absolute value of **B**
B*	critical value of magnetic field
I	arc current
L	z-position of the anode
Q	mass flow rate of plasma gas
R	dimensionless position, $\mathbf{R} = \mathbf{r}/\zeta$
T	dimensionless time, $T = t/\tau$
X	dimensionless x-position, $X = x/\zeta$
Y	dimensionless y-position, $Y = y/\zeta$
Z	dimensionless z-position, $Z = z/\zeta$
b	unit vector, $\mathbf{b} = \mathbf{B}/B$
j	current density of arc (vector)
r	position of plasma gas (vector)
t	time
v	velocity of plasma gas (vector)
v_o	initial velocity of plasma gas
x	x-component of **r**
y	y-component of **r**
z	z-component of **r**
α	proportional constant
λ	operating variable, $\lambda = IB/Q$
θ	intersection angle of **B** to z-axis
ρ	density of plasma gas
ζ	characteristic length, $\zeta = -v_o/\lambda$
τ	characteristic time, $\tau = 1/\lambda$

Table 1. List of main parameters used in the modelling

2. Momentum equation for the plasma gas

The arrangement of the theoretical model is illustrated in Figure 3. A transferred arc is generated between the anode and the cathode in the torch. Plasma forming gas is ionized in the torch and ejected from the exit of the torch nozzle at the velocity v_o. It is assumed that the magnetic field **B** is uniform in space and it has no y-component ($B_y = 0$). In an alternating magnetic field, the intersection angle between the field vector and z-axis changes from θ for a certain half period to $(\theta + \pi)$ for another half period, since **B** reverses its direction at the time interval of the half period. The frequency (f) of the alternating field is also assumed to be so small that the ionized gas may travel as if the field was in a steady state during the flight from
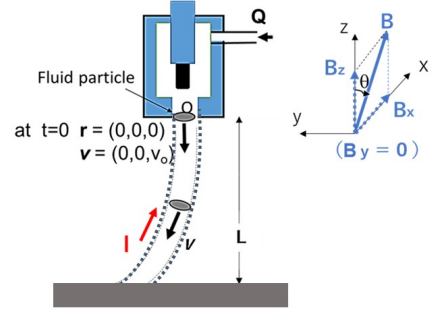

Figure 3. Schematic illustration of the the model.

the torch to the anode. The flight time of the plasma gas is estimated to be L/v_o in order of magnitude. Typically, $L/v_o \sim 10^{-3}$ s as the distance (L) and the velocity (v_o) are 10^{-1} m and 10^2 m s^{-1} respectively. Therefore, if f is restricted in the range of 100 Hz or less, the assumption of the steady field can be satisfied [5].

The key idea in the present modelling is that the trajectory of the plasma gas motion represents the arc profile, since the arc current has to pass along the stream line of the plasma gas which is electrically conductive. The momentum equation of the plasma gas is expressed as

$$\rho \frac{\mathrm{d}\mathbf{v}}{\mathrm{d}t} = \mathbf{j} \times \mathbf{B}. \tag{1}$$

Using a unit vector **b**, the magnetic field is written as

$$\mathbf{B} = B\mathbf{b}. \tag{2}$$

When intersection angle equals θ,

$$\mathbf{b} = (b_x, b_y, b_z) = (\sin\theta, 0, \cos\theta). \tag{3}$$

Based on the fundamental idea used in the modelling, **j** is expressed as

$$\mathbf{j} = -\alpha\mathbf{v} \tag{4}$$

where α is a positive proportional constant. A minus sign results from the anti-parallel relation between the plasma gas motion and the arc current. Considering the continuity of the gas flow and that of the arc current, the following relation is obtained

$$I = \alpha \frac{Q}{\rho}. \tag{5}$$

Then the equation (1) is rewritten as

$$\frac{\mathrm{d}\mathbf{v}}{\mathrm{d}t} = -\lambda\left(\mathbf{v} \times \mathbf{b}\right), \tag{6}$$

where

$$\lambda = \frac{IB}{Q}. \tag{7}$$

Since

$$\mathbf{v} = \frac{\mathrm{d}\mathbf{r}}{\mathrm{d}t}, \tag{8}$$

the momentum equation is expressed as

$$\frac{\mathrm{d}^2\mathbf{r}}{\mathrm{d}t^2} = -\lambda \left(\frac{\mathrm{d}\mathbf{r}}{\mathrm{d}t} \times \mathbf{b} \right). \tag{9}$$

The plasma gas starts from the torch exit at $t = 0$, with initial velocity v_o directed downward along z-axis. The trajectory of the plasma gas is obtained by solving the momentum equation using a Lagrangian method. Initial conditions at $t = 0$ are given as

$$(\mathbf{r})_{t=0} = (x, y, z)_{t=0} = (0, 0, 0) \tag{10}$$

$$\left(\frac{\mathrm{d}\mathbf{r}}{\mathrm{d}t} \right)_{t=0} = \left(\frac{\mathrm{d}x}{\mathrm{d}t}, \frac{\mathrm{d}y}{\mathrm{d}t}, \frac{\mathrm{d}z}{\mathrm{d}t} \right)_{t=0} = (0, 0, v_o), \tag{11}$$

and

$$\left(\frac{\mathrm{d}^2x}{\mathrm{d}t^2}, \frac{\mathrm{d}^2y}{\mathrm{d}t^2}, \frac{\mathrm{d}^2z}{\mathrm{d}t^2} \right)_{t=0} = (0, -\lambda v_o sin\theta, 0). \tag{12}$$

When the applied magnetic field is alternating, λ in equation (9) and initial condition (12) varies its magnitude depending on the field strength B. And the vector $\mathbf{b}$ changes its direction from θ for a half period to $(\theta + \pi)$ for another half period. Therefore, for another half period, equation (3) and equation (12) should be replaced by the following equations

$$\mathbf{b} = (sin(\theta + \pi), 0, cos(\theta + \pi)) = (-\sin\theta, 0, -\cos\theta) \tag{13}$$

and

$$\left(\frac{\mathrm{d}^2x}{\mathrm{d}t^2}, \frac{\mathrm{d}^2y}{\mathrm{d}t^2}, \frac{\mathrm{d}^2z}{\mathrm{d}t^2} \right)_{t=0} = (0, \lambda v_o sin\theta, 0). \tag{14}$$

3. Non-dimensional analysis

3.1. Definition of characteristic length and time

In an alternating magnetic field, the arc changes its profile with B. To know the variation of arc, it is required to solve the differential equation (9) many times for various λ. To avoid such troublesome, non-dimensional analysis was proposed in this work. Here, dimensionless time (T) and dimensionless position ($\mathbf{R}$) were considered using characteristic time (τ) and length (ζ). The time was normalized by the characteristic time and converted into the dimensionless time as

$$T = t/\tau. \tag{15}$$

The position was normalized by the characteristic length and converted into the dimension position as

$$\mathbf{R} = \mathbf{r}/\zeta \tag{16}$$

or

$$X = x/\zeta, Y = y/\zeta, Z = z/\zeta. \tag{17}$$

Where the characteristic time and length were defined respectively as

$$\tau = 1/\lambda = Q/(IB) \tag{18}$$

and

$$\zeta = -v_o\lambda = -(v_oQ)/(IB). \tag{19}$$

3.2. Dimensionless momentum equation

Using the dimensionless time and the dimensionless position, the momentum equation (9) was transformed into the following dimensionless equation as

$$\frac{\mathrm{d}^2\mathbf{R}}{\mathrm{d}T^2} = \left(\frac{\mathrm{d}\mathbf{R}}{\mathrm{d}T} \times \mathbf{b} \right). \tag{20}$$

And the initial conditions presented in equations (10-12) were transformed into

$$(\mathbf{R})_{T=0} = (X, Y, Z)_{T=0} = (0, 0, 0), \tag{21}$$

$$\left(\frac{\mathrm{d}\mathbf{R}}{\mathrm{d}T} \right)_{T=0} = \left(\frac{\mathrm{d}X}{\mathrm{d}T}, \frac{\mathrm{d}Y}{\mathrm{d}T}, \frac{\mathrm{d}Z}{\mathrm{d}T} \right)_{T=0} = (0, 0, -1) \tag{22}$$

and

$$\left(\frac{\mathrm{d}^2X}{\mathrm{d}T^2}, \frac{\mathrm{d}^2Y}{\mathrm{d}T^2}, \frac{\mathrm{d}^2Z}{\mathrm{d}T^2} \right)_{T=0} = (0, \sin\theta, 0). \tag{23}$$

To calculate the trajectory of the plasma gas motion, the dimensionless momentum equation (20) was decomposed into three scalar equations. For the X-component,

$$\frac{\mathrm{d}^2X}{\mathrm{d}T^2} = -\frac{\mathrm{d}Y}{\mathrm{d}T} \cos\theta. \tag{24}$$

For the Y-component and the Z-component were respectively rewritten as

$$\frac{\mathrm{d}^2Y}{\mathrm{d}T^2} = -\frac{\mathrm{d}Z}{\mathrm{d}T} \sin\theta + \frac{\mathrm{d}X}{\mathrm{d}T} \cos\theta, \tag{25}$$

and

$$\frac{\mathrm{d}^2Z}{\mathrm{d}T^2} = -\frac{\mathrm{d}Y}{\mathrm{d}T} \sin\theta. \tag{26}$$

While scalar product of the vector $\mathbf{b}$ to the vector equation (20) yielded the following relation

$$\frac{\mathrm{d}}{\mathrm{d}T} \left(\frac{\mathrm{d}X}{\mathrm{d}T} \sin\theta + \frac{\mathrm{d}Z}{\mathrm{d}T} \cos\theta \right) = 0. \tag{27}$$

Considering the initial condition at $T = 0$, equation (27) lead to

$$\frac{\mathrm{d}X}{\mathrm{d}T} \sin\theta + \frac{\mathrm{d}Z}{\mathrm{d}T} \cos\theta = -\cos\theta. \tag{28}$$

Taking the above relation into account, the simultaneous equations (24-26) were rearranged into the following three third-order linear ordinary differential equations

$$\frac{\mathrm{d}^3X}{\mathrm{d}T^3} + \frac{\mathrm{d}X}{\mathrm{d}T} + \sin\theta \cos\theta = 0, \tag{29}$$

$$\frac{\mathrm{d}^3Y}{\mathrm{d}T^3} + \frac{\mathrm{d}Y}{\mathrm{d}T} = 0, \tag{30}$$

and

$$\frac{\mathrm{d}^3Z}{\mathrm{d}T^3} + \frac{\mathrm{d}Z}{\mathrm{d}T} + \cos^2\theta = 0. \tag{31}$$

As you notice, all the experimental parameters except θ disappear in these differential equations and initial conditions. Therefore, the trajectory of the plasma gas in the dimensionless Cartesian coordinate system can be calculated indifferently to the operating conditions such as λ and v_o.

4. Solution in dimensionless coordinates

4.1. Trajectory in the perpendicular field

To solve the differential equations (29-31) with the initial conditions (21-23), the commercial software Mathematica[7] was used. In a perpendicular magnetic field ($\theta = \pi/2$), differential equations became quite simple as

$$\frac{d^3X}{dT^3} + \frac{dX}{dT} = 0, \tag{32}$$

$$\frac{d^3Y}{dT^3} + \frac{dY}{dT} = 0 \tag{33}$$

and

$$\frac{d^3X}{dT^3} + \frac{dX}{dT} = 0. \tag{34}$$

Initial conditions were

$$(X, Y, Z)_{T=0} = (0, 0, 0), \tag{35}$$

$$\left(\frac{dX}{dT}, \frac{dY}{dT}, \frac{dZ}{dT}\right)_{T=0} = (0, 0, -1) \tag{36}$$

and

$$\left(\frac{d^2X}{dT^2}, \frac{d^2Y}{dT^2}, \frac{d^2Z}{dT^2}\right)_{T=0} = (0, 1, 0). \tag{37}$$

The trajectory obtained in dimensionless coordinate system was represented in Figure 4. At $T = 0$, the plasma gas started from the origin$(0, 0, 0)$ of the dimensionless Cartesian coordinate system (X, Y, Z) and it moved along a circle on a Y-Z plane in the clock-wise direction with the increase of T.

While for $\theta = 3\pi/2$, equations (32-34) and initial conditions (35-36) were same but the third initial condition was different from equation (37). It was described as

$$\left(\frac{d^2X}{dT^2}, \frac{d^2Y}{dT^2}, \frac{d^2Z}{dT^2}\right)_{T=0} = (0, -1, 0). \tag{38}$$

The resulting trajectory was illustrated in Figure 5. Both trajectories shown in Figure 4 and Figure 5 are mirror symmetrical with respect to a X-Z plane at Y=0.

4.2. Trajectory in the oblique field

In case of an oblique field ($\theta \neq \pi/2$), differential equations (29-31) were solved under the initial conditions (21-23) for various values of θ. The plasma gas described a helical line as its trajectory. The projection of the helix in the plane normal to **b** was a circle with radius equal to $\sin\theta$. The center of the circle moved in the direction of $-\mathbf{b}$ (anti-parallel to **b**) at the constant velocity equal to $\cos\theta$. For $0 < \theta < \pi/2$, the trajectories in the magnetic field with the intersection angle θ and that with $\theta + \pi$ were illustrated in Figure 6 and in Figure 7 respectively. These two trajectories were mirror symmetrical to each other with respect to a X-Z plane at Y=0.
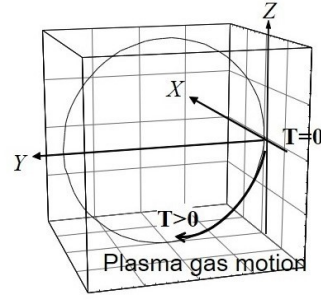

Figure 4. The movement of the plasma gas under the perpendicular field ($\theta = \pi/2$) in the dimensionless space.
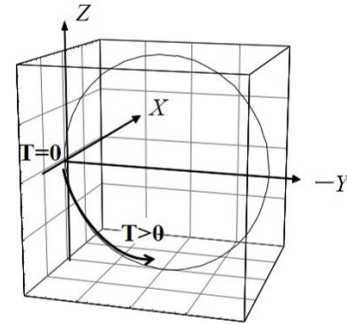

Figure 5. The movement of the plasma gas under the perpendicular field ($\theta = 3\pi/2$) in the dimensionless space

The trajectory in the magnetic field with $\theta + \pi/2$ and that with $\theta + 3\pi/2$ were also calculated. It was known that the trajectories in the field with θ and with $\theta + \pi/2$ were mirror symmetrical with respect to a Y-Z plane at X=0. The trajectory in the field with $\theta + \pi$ and that in the field with $\theta + 3\pi/2$ were also in similar symmetry.

5. Arc motion in real coordinates

The trajectories of the plasma gas in a real space are obtained by the inverse transformation of the dimensionless coordinates (X, Y, Z) to the dimensional ones (x, y, z) using equations (17-19). Arc profile is represented by the trajectory of the plasma gas from the torch exit to the anode. Numerical calculations on the deformation of arc profiles with the change of B were carried out under the operating conditions $Q = 3.0 \times 10^{-4}\,\mathrm{kg\,s^{-1}}$, $I = 90\,\mathrm{A}$, and $v_o = 80\,\mathrm{m^{-1}}$. It was assumed that the anode plane located at the position of $z = -L = -5.0 \times 10^{-2}\,\mathrm{m}$.

5.1. Arc motion in the perpendicular field

In the perpendicular magnetic field ($\theta = \pi/2$), the arc profiles for various magnitude of B are obtained by the inverse transformation along the circle shown in Figure 4. Deformations of the arc profiles with the change of B are illustrated in Figure 8. For $B = 0$, the position of the arc root on the anode locates at A_0 and it moves along the y-axis through A_1 and A_2
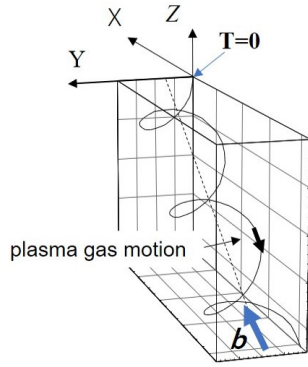
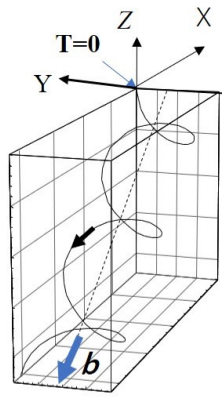*Figure 6. The movement of the plasma gas under the oblique field $(0 < \theta < \pi/2)$ in the dimensionless space*

Figure 8. The movement of the plasma gas under the perpendicular field of $\theta = \pi/2$ in the real space

Figure 7. The movement of the plasma gas under the oblique field $(\pi < \theta < 3\pi/2)$ in the dimensionless space

Figure 9. The movement of the plasma gas under the perpendicular field of $\theta = 3\pi/2$ in the real space

to A^* with the increase of B. If the magnitude of B is larger than this critical strength B^*, the arc goes up without contact with the anode. In such situation, the arc becomes unstable as the circuit of the arc current destroys. The critical magnetic field is expressed as

$$B^* = \frac{v_o Q}{IL} \tag{39}$$

The maximum displacement of the anode root A^* equals L.

In the perpendicular field for $\theta = 3\pi/2$, the arc profiles for various magnitude of B are shown in Figure 9. The whole view of the arc oscillation driven by alternating magnetic field is shown in Figure 10. The arc oscillates in a flat y-z plane.

5.2. Arc motion in the oblique field

The arc profiles in the oblique magnetic field with the intersection angle of $\theta = \pi/6$ are shown in Figure 11, where the helical motion in Figur 6 is replaced by the inverse transformations into different helical motions with various values of B. The plasma gas travels on the three dimensional curved plane. The
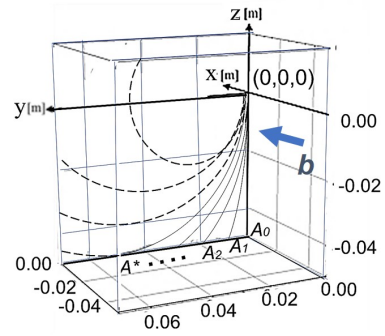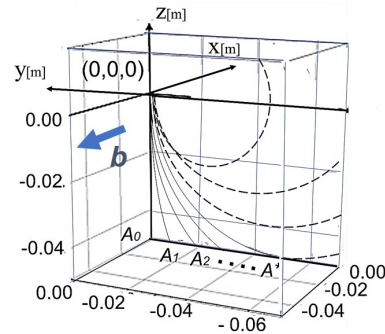
arc root on the anode plate moves in the counter-clockwise direction with the increase of B. When the intersection angle of the field is $\theta = 7\pi/6$, the arc profiles are mirror symmetric with respect of a x-z plane at $y = 0$. The whole view of the oscillatory arc in the oblique alternating magnetic field is illustrated in Figure 12.

5.3. Experimental confirmation

Experimental observation was performed under the operating conditions $Q = 3.0 \times 10^{-4}\,\text{kg s}^{-1}$, $I = 90\,\text{A}$ and $v_o = 80\,\text{m}^{-1}$. The sinusoidal alternating magnetic field was imposed at the frequency $f = 50\,\text{Hz}$, and its amplitude was $B = 2.0 \times 10^{-3}\,\text{T}$. The oscillatory arc in the perpendicular field and that in the oblique field were shown in Figure 13. Although many simplified assumptions were used in the modelling, experimental results confirmed the validity of the theoretical consideration.

6. Conclusions

The authors have developed a heat treatment system with the magnetically driven arc. To improve the system, arc behaviours in various operating conditions were investigated theoretically. In the simulation of the arc motion, non-dimensional analysis was proposed, where the momentum equation for the plasma gas was converted into the dimensionless equation using the characteristic time and length. When these
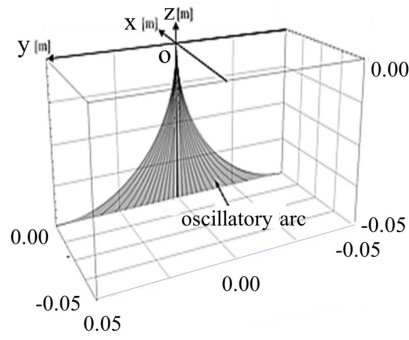
Figure 10. Oscillatory motion of the arc under an alternating field imposed perpendicularly
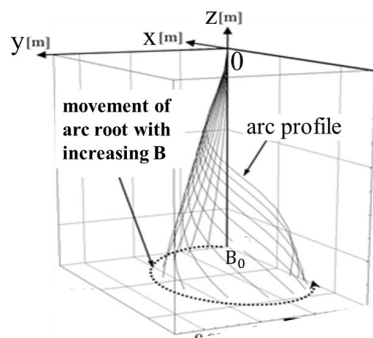

Figure 11. The movement of the plasma gas under the oblique field ($\theta = \pi/6$) in the real space

Figure 12. Oscillatory motion of the arc under an alternating magnetic field imposed obliquely
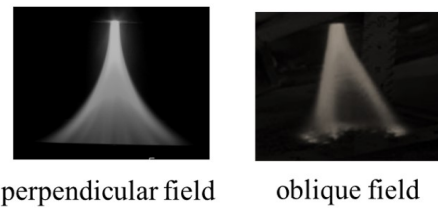
Figure 13. Oscillatory motion of the arc in the perpendicular field and that in the oblique field

characteristic time and length were defined pertinently, the dimensionless momentum equation became independent of the operating conditions B, Q, I and v_o. Therefore, the trajectory of the plasma gas motion calculated in this dimensionless coordinate system was also independent of the operating parameters. The arc motions in the real space were obtained by the inverse transformations of the trajectory in dimensionless coordinates system.

Main results obtained from the numerical calculations are as follows: In an alternating magnetic field applied perpendicularly, the arc oscillates on a flat plane. The amplitude of its oscillatory motion increases with the increase of the magnetic field strength. But the arc becomes unstable when B exceeds the critical strength equal to Qv_o/IL. The arc describes a part of a circle, the radius of which depends on B. While the magnetic field is applied obliquely to the arc, the arc oscillates on a curved plane. The arc describes a helical line, the curvature of which also depends on B. Theoretical predictions were confirmed by the experimental observations.

References

[1] J.E.Harry and D.Goodwin. Surface heattreatment using a plasma torch with a magnetically traversed arc. In *4th Int. Conf. on Advance in Welding Processes*, pages 181–184, 1978.
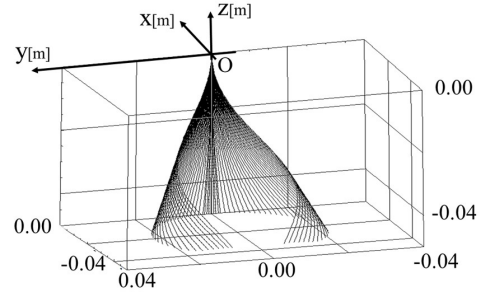
[2] K.Takeda. Oscillating plasma arc by external ac magnetic field. In O. Solonenko, editor, *Proceedings Int. Workshop on Plasam Jet in the Development of New Materials Technology*, pages 486–492, 1990.

[3] Y.Maruki T.Yamamoto T.Toh, J.Tanaka and K.Takeda. Magnetohydrodynamic simulation of dc arc plasma under ac magnetic field. *ISIJ International*, 45(7):947–953, 2005.

[4] K.Takeda Y.Noguchi R.Akiho, M.Sugimoto and T.Miura. The development of a heat treatment system using a magnetically driven arc. *Transactions of the JSME*, 79(806):3979–3992, 2013.

[5] K.Takeda H.Okubo and M.Sugimoto. Time response of arc driven by alternating magnetic field. In 13th High-Tech Plasma Processes Conference, editor, *Journal of Physics: conference Series 505*, pages 1–10, 2014.

[6] K.Takeda R.Akiho and M.Sugimoto. Arc motion in an obliquely imposed alternating magnetic field. In 12th High-Tech Plasma Processes Conference, editor, *Journal of Physics: conference Series 406*, pages 1–10, 2012.

[7] S. Wolfram. *The Mathmatica book.* 3rd edition. Wolfram Research Inc. Champaign, 1998.